Available online at www.sciencedirect.com
SCIENCE DIRECT®

Nuclear Instruments and Methods in Physics Research A 507 (2003) 459–463

NUCLEAR INSTRUMENTS & METHODS IN PHYSICS RESEARCH
Section A

www.elsevier.com/locate/nima

Image charge undulator

Yuhong Zhang*, Yaroslav Derbenev, Rui Li

Center for Advanced Studies of Accelerators, Thomas Jefferson National Accelerator Facility, 12000 Jefferson Ave., Newport News, VA 23606, USA

Abstract

A relativistic electron beam moving close to periodic grating surfaces may undergo undulating motion due to its image charge wakefields. This motion can be a mechanism for producing hard incoherent or coherent radiation. A new device, an image charge undulator, is proposed to realize this mechanism. We demonstrate the physics principle of this device by a two-dimensional model with an infinitely long uniform sheet current. The new undulator could be employed for constructing a single-pass, high-intensity, compact-size and ultra-short-wavelength light source.

1. Introduction

Since Smith and Purcell's landmark experiment [1], radiation from relativistic electrons passing near metal grating surfaces has been continuously interesting to many physicists, mainly due to the hope of creating compact-size ultra-short wavelength light sources based on this effect. The Smith–Purcell effect is commonly explained as refraction of electric fields carried by relativistic electrons (point charge or short bunch) by an open grating surface. Recently, Kim and Song [2] pointed out possible enhancements of Smith–Purcell radiations for a longitudinally modulated electron bunch and proposed a refraction-based SASE FEL process.

In this paper, we report on the possibility of generating incoherent or coherent hard radiation using a mechanism other than field refraction, namely the transverse undulating motion of electrons in wakefields produced by an electron beam when moving near a grating structure.

2. Physics principle

An electron beam near a metal surface produces an electric polarization (image charge) of the surface, which applies a Lorentz force back on the beam. The image charge wakefields become wiggler type fields when the surface is periodically alternating like a grating. Under these forces, the electron beam undergoes undulating motion and emits radiations just like in a conventional magnetic undulator. Therefore, wave amplification and lasing can happen. To enhance the wakefield and also stabilize the beam, we close the grating structure by a second identical surface as shown in Fig. 1. We name such an asymmetric periodic structure as an image charge undulator (ICU). This planar ICU can also be modified to a helical grating channel (with a round beam) to generate circularly polarized photons. The undulating

*Corresponding author.
E-mail address: yzhang@jlab.org (Y. Zhang).

0168-9002/03/$ - see front matter
doi:10.1016/S0168-9002(03)00966-5

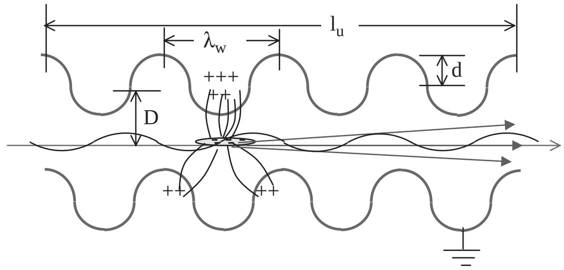

Fig. 1. Schematic drawing of 2-D image charge undulator.

mechanism can be clearly seen for a model of a uniform sheet beam (of surface density σ_0) in a two-dimensional (2D) grating structure. Here, the image charge wakefields are given by static solutions, at constant charge and current densities. The magnetic field being parallel to the surface is not changed from the free space case by the grating, while the electric field is deformed getting an alternating part due to periodic polarization of the surface. The transverse wakefield (excluding the field of sources) has the general form

$$E_x(x,z) = \sum_{n=1}^{+\infty} E_{xn}(x)\sin(nk_w z + \phi_{xn}) \tag{1}$$

to reflect the periodicity in the z direction, where ϕ_{xn} is a phase factor, $k_w = 2\pi/\lambda_w$ and λ_w is the undulator period. Apart from a numerical factor which only depends on the grating geometry, wakefields of the ICU are proportional to $E_0 = 2\pi\sigma_0$, the static electric field of the uniform sheet charge in free space. Normally, higher harmonic terms decay fast and the above expansions are largely dominated by the first several nonzero terms. Keeping only the first term, we obtain from the electron equation of motion that

$$v_x(z) \simeq \frac{cK}{\gamma_0}\cos(k_w z + \varphi_0), \quad K = \frac{eE_{x1}(0)}{mv_0^2 k_w} \tag{2}$$

where v_0 is the electron velocity and γ_0 is the Lorentz factor. Here $E_{x1}(x) \simeq E_{x1}(0)$ because $x(z)$ is very small for high energy electron beams. The resonance frequency for an FEL process, according to the well-developed FEL theory [3], is $\lambda = \lambda_w(1+\frac{1}{2}K^2)/2\gamma_0^2$. For an electron bunch of a finite length (σ_z) but much longer than the grating period, the wakefield can be represented by a quasi-static model, i.e., a static solution following the bunch. For a short bunch, $\sigma_z \leqslant \lambda_w$, wakefield results from bunch field diffraction on crests of grating surface. It should be noted that K varies along the bunch of nonuniform charge density. However, other than a widening of the SASE spectrum, this inhomogeneity does not present a serious challenge for realization of SASE FEL even at large K, due to a quasi-local character of the amplification process. As an example, let us estimate the undulating motion for a flat beam of 200 MeV energy in an ICU of 30 μm period. The flat bunch is 100 μm long, 300 μm wide and 4 μm thick, and contains 6×10^{10} electrons (total charge 10 nC). Other dimensions of the ICU, i.e., grating depth d and separation of two grating $2D$, are typically equal or close to the grating period. Assuming the geometric-dependent numerical factor is in order of 1, we found $K \sim 0.2$, which is equivalent to 60 T peak magnetic field in a "conventional" undulator. The resonance frequency associated to this ICU is about 1 Å, an X-ray, and gain length [3] is around 2 cm.

3. A simple 2D model

The key quantity for an ICU is amplitudes of image charge wakefield for a given grating geometry. In this section, we present an analytical calculation of image charge wakefields for the simple geometry shown in Fig. 2. This 2D model can be viewed as a 2D waveguide (of vertical size $2D$) attached by two sets of uniformly distributed identical 2D rectangular cavities (width L and depth d). Adjacent cavities are separated by a distance L. Thus, the period of this ICU is $2L$. Both waveguide and cavities are made of perfectly conducting material. A uniform sheet current is passing through the center of the ICU ($x=0$). We further assume the undulator and current are very long so boundary effects are negligible. To find the image charge wakefields, we divide the space inside the undulator into three distinct regions: (I) upper cavity region ($D<x<D+d$), (II) waveguide region ($-D<x<D$) and (III) lower cavity region ($-D-d<x<-D$), then solve the Maxwell equations for each region separately. The only nonzero

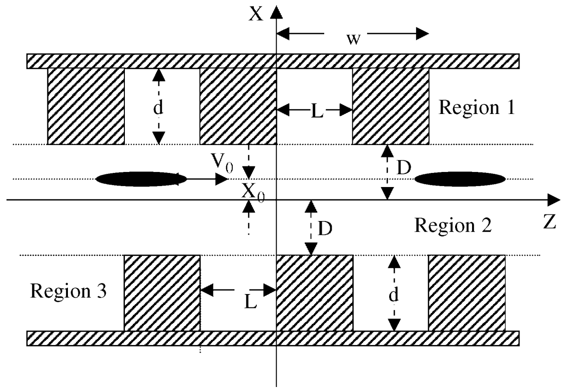

Fig. 2. 2-D Image Charge Undulator made of 2-D waveguide and 2-D rectangular shape cavities.

field components are E_x, E_z and B_y. We construct fields in the frequency domain in the upper cavity region in terms of single cavity modes as follows:

$$E_x^{\mathrm{I}}(x,z,\omega)=\sum_{\mu} H_{\mu}^{\mathrm{I}}(x,z)\sum_{n=0}^{+\infty} C_{\mu n}(\omega)\frac{k_n}{q_n} \times \cos q_n(D+d-x) \times \sin k_n(z+2\mu L) \tag{3}$$

$$E_z^{\mathrm{I}}(x,z,\omega)=\sum_{\mu} H_{\mu}^{\mathrm{I}}(x,z)\sum_{n=0}^{+\infty} C_{\mu n}(\omega) \times \sin q_n(D+d-x) \times \cos k_n(z+2\mu L) \tag{4}$$

where $k_n=n\pi/L$ and $q_n=(\omega^2/c^2-k_n^2)^{1/2}$. Function $H_{\mu}^{\mathrm{I}}(x,z)$ defines the boundary of the μth upper cavity, i.e., it equals 1 for $(2\mu L<z<(2\mu+1)L, D<x<D+d)$ and zero elsewhere. The above fields already satisfy boundary conditions on three perfect conducting surfaces of the cavity. Coefficients $C_{\mu n}(\omega)$ will be determined by matching fields across the cavity openings ($x=D$). The fields in the lower cavity region can be constructed in a similar way; a different set of coefficients $D_{\mu n}(\omega)$ will be also determined by matching boundary conditions on the interface $x=-D$. In the second (waveguide) region, the electric fields are

$$E_x^{\mathrm{II}}(x,z,\omega)=E_x^{s}(x,z,\omega)+E_x^{ns}(x,z,\omega) \tag{5}$$

$$E_z^{\mathrm{II}}(x,z,\omega)=E_z^{s}(x,z,\omega)+E_z^{ns}(x,z,\omega). \tag{6}$$

The first part, which satisfies the Maxwell equations with source (surface charge density σ_0), are

$$E_x^{s}(x,z,\omega)=s(x)G\left(x_>,\frac{\omega}{v_0}\right)\cosh\frac{\omega(D+x_<)}{v_0\gamma_0} \tag{7}$$

$$E_z^{s}(x,z,\omega)=-\frac{i}{\gamma_0}G\left(x_>,\frac{\omega}{v_0}\right)\sinh\frac{\omega(D+x_<)}{v_0\gamma_0} \tag{8}$$

where

$$G(x,k)=\frac{4\pi\sigma(k)}{v_0}\frac{\sinh(k/\gamma_0)(D-x)}{\sinh(k/\gamma_0)2D}. \tag{9}$$

Here $s(x)$ is a sign function defined as 1 or -1 when x is either greater or less than zero, and $x_<$ and $x_>$ equal the smaller or bigger one among x and 0 (the position of the sheet beam), respectively. The second parts of (5) and (6), which satisfy *sourceless* Maxwell equations, are

$$E_x^{ns}(x,z,\omega)=\int_{-\infty}^{+\infty}\frac{\mathrm{d}k}{2\pi}\mathrm{e}^{\mathrm{i}kz}\frac{\mathrm{i}k}{q}[A(k,\omega)\cos q(D+x) - B(k,\omega)\cos q(D-x)] \tag{10}$$

$$E_z^{ns}(x,z,\omega)=\int_{-\infty}^{+\infty}\frac{\mathrm{d}k}{2\pi}\mathrm{e}^{\mathrm{i}kz}[A(k,\omega)\sin q(D+x) + B(k,\omega)\sin q(D-x)]. \tag{11}$$

Here, $A(k,\omega)$ and $B(k,\omega)$ are two sets of expansion coefficients. While the longitudinal electric field must be continuous on the entire interfaces ($x=\pm D$) between the waveguide and the upper/lower cavities, the transverse electric field is only continuous at the cavity openings. By matching these boundary conditions we obtain four sets of equations involving four sets of coefficients $A(k,\omega)$, $B(k,\omega)$, $C_{\mu n}(\omega)$ and $D_{\mu n}(\omega)$. Eliminating $C_{\mu n}(\omega)$ and $D_{\mu n}(\omega)$, and using the following (cavity) mode expansions [4]:

$$A(k,\omega)=\sum_{\mu,n}\mathrm{e}^{\mathrm{i}(\omega/v_0-k)2\mu L}a_{\mu n}(\omega)M_{\mu n}(k,\omega) \tag{12}$$

$$B(k,\omega)=\sum_{\mu,n}\mathrm{e}^{\mathrm{i}(\omega/v_0-k)(2\mu+1)L}b_{\mu n}(\omega)M_{\mu n}(k,\omega) \tag{13}$$

where

$$M_{\mu n}=2L\frac{G(0,\omega/v_0)}{\sin 2qD}I_{sn}\left(\frac{\omega}{v_0}L\right) \times I_{cn}(kL)\frac{q_n}{k_n}\tan q_n d \tag{14}$$

$$I_{sn}(\eta) = \frac{n\pi[1-(-1)^n e^{i\eta}]}{(n\pi)^2 - \eta^2} \tag{15}$$

$$I_{cn}(\eta) = \frac{i\eta[1-(-1)^n e^{-i\eta}]}{(n\pi)^2 - \eta^2} \tag{16}$$

we obtain the following two sets of linear equations:

$$a_{\mu n} = 1 + \sum_{\nu} \sum_{m=0}^{+\infty} [\Gamma_{nm}^{(\mu-\nu)} a_{\mu m} - \Lambda_{nm}^{(\mu-\nu)} b_{\nu m}] \tag{17}$$

$$b_{\mu n} = 1 + \sum_{\nu} \sum_{m=0}^{+\infty} [\Gamma_{nm}^{(\mu-\nu)} b_{\mu m} - \Lambda_{nm}^{(\mu-\nu)} a_{\nu m}] \tag{18}$$

where

$$\Gamma_{nm}^{(\alpha)}(\omega) = 2L \frac{I_{sm}((\omega/v_0)L)}{I_{sn}((\omega/v_0)L)} \frac{q_m}{k_m} \tan q_m d \int_{-\infty}^{+\infty} \frac{dk}{2\pi} ik \times \frac{I_{sn}(kL) I_{cm}(kL)}{q \tan 2qD} e^{i(k-\omega/v_0)2\alpha L} \tag{19}$$

$$\Lambda_{nm}^{(\alpha)}(\omega) = 2L \frac{I_{sm}((\omega/v_0)L)}{I_{sn}((\omega/v_0)L)} \frac{q_n}{k_m} \tan q_m d \int_{-\infty}^{+\infty} \frac{dk}{2\pi} ik \times \frac{I_{sn}(kL) I_{cm}(kL)}{q \sin 2qD} e^{i(k-\omega/v_0)(2\alpha+1)L} \tag{20}$$

are elements of the coupling matrix between the nth mode of the μth cavity on one side of the ICU and the mth mode of the νth cavity on the same or opposite side. For an infinitely long ICU, due to the translational symmetry, $a_{\mu n}(\omega)$ and $b_{\mu n}(\omega)$ should be independent of cavity index μ, i.e., $a_{\mu n}(\omega) = a_n(\omega)$, $b_{\mu n}(\omega) = b_n(\omega)$. It further can be shown from Eqs. (17) and (18) that $a_n(\omega) = b_n(\omega)$. Thus,

$$a_n(\omega) = 1 + \sum_{m=0}^{+\infty} [\Gamma_{nm}(\omega) - \Lambda_{nm}(\omega)] a_m(\omega) \tag{21}$$

where the new matrix elements are

$$\Gamma_{nm} = \sum_{\alpha=-\infty}^{+\infty} \Gamma_{nm}^{(\alpha)}, \quad \Lambda_{nm} = \sum_{\alpha=-\infty}^{+\infty} \Lambda_{nm}^{(\alpha)}. \tag{22}$$

Now we use the condition of uniform charge density, $\sigma(z) = \sigma_0$, in the frequency domain, $\sigma(\omega) = \sigma_0 2\pi\delta(\omega)$; thus only $\omega = 0$ terms have contributions to the image charge wakefields. It is straightforward to show that both transverse and longitudinal image charge wakefields are periodic (the period is $\lambda_w = 2L$) over z. Therefore, they can be expanded in terms of Fourier series as (1). Coefficients $E_{xn}(x)$ and $E_{zn}(x)$, and phase factors $\phi_{xn}(x)$ and $\phi_{zn}(x)$ can be calculated analytically. In particular, near the undulator center, the image charge field is reduced to

$$E_x^{ns}(0,z) = E_0 \sum_{n=0}^{+\infty} N_{x2n+1} \sin(2n+1)k_w z \tag{23}$$

$$E_z^{ns}(0,z) = E_0 \sum_{n=1}^{+\infty} N_{z2n} \sin 2nk_w z \tag{24}$$

where $E_0 = 2\pi\sigma_0$ and numerical factors are

$$N_{x2n+1} = -\frac{a_{2n+1}(0) \tanh(2n+1)\pi d/L}{(n+\frac{1}{2})\pi \sinh(2n+1)\pi D/L} \tag{25}$$

$$N_{z2n} = \frac{1}{\pi^2 \cosh 2n\pi D/L} \times \sum_{m=1}^{+\infty} \frac{a_{2m+1}(0) \tanh(2m+1)\pi d/L}{(m+\frac{1}{2})[(m+\frac{1}{2})^2 - n^2]}. \tag{26}$$

The fact that all terms above are proportional to a factor $\tanh(2n+1)d/L$ implies that the image charge forces vanish when all cavities disappear ($d = 0$). On the other hand, by being inversely proportional to $\sin(2n+1)\pi D/L$, the transverse image charge wakefields would be enhanced when the vertical size D decreases.

4. Discussion

ICUs possess several features for light source applications. Apart from the difference in source of undulating force, an ICU is much like a magnetic undulator; hence, the well-developed theories of incoherent and coherent radiation can be applied to ICUs. With current technology, one effectively can construct a compact size light source for very short wavelength by manufacturing very fine grating structure. One can also load several IUCs together for one light source application. IUCs on helical grating channel seem suitable to produce the intense circularly polarized gamma rays from high-energy electron beams for various use. There are also several significant technical challenges one needs to overcome in order to fully realize the power of this new FEL mechanism. Among them are beam alignment, removing fairly large amount of heat from grating surfaces, flat electron beams of a small X-emittance. To meet these challenges, current technologies are under active evaluation and new schemes have also been proposed. For example, the recently proposed round-to-flat electron beam source [5] appears well conjuncted with 2D ICU. We are grateful to J. Boyce, B. Wojtsekhowski and A. Mikhailichenko for discussions on ICU technology and applications, and also to J. Boyce for permission to use Fig. 1.

References

[1] S.J. Smith, E.M. Purcell, Phys. Rev. 92 (1953) 1069.
[2] K. Kim, S. Song, Nucl. Instr. and Meth. A 475 (2001) 153.
[3] E.L. Saldin, et al., The Physics of Free Electron Lasers, Springer, Berlin, 2000.
[4] S.A. Heifets, S.A. Kheifets, Phys. Rev. D 39 (1989) 960.
[5] A. Burov, S. Nagaitsev, Y. Derbenev, Phys. Rev. E 66 (2002) 016 503.